AGU ADVANCING EARTH AND SPACE SCIENCES

Geophysical Research Letters

RESEARCH LETTER
10.1029/2023GL107678

Deforestation-Driven Increases in Shallow Clouds Are Greatest in Drier, Low-Aerosol Regions of Southeast Asia

Gabrielle R. Leung[1], **Leah D. Grant**[1], **and Susan C. van den Heever**[1]

[1]Department of Atmospheric Science, Colorado State University, Fort Collins, CO, USA

Abstract Anthropogenic activity drives extensive tropical deforestation, particularly in Southeast Asia where 16% of total forest cover was lost between 2000 and 2020. While land surface changes significantly affect the atmosphere, their net impact on convective clouds is not well-constrained. Here, we use satellite data to demonstrate long-term deforestation in Southeast Asia robustly alters cloud properties and provide the first observational evidence that the magnitude of this response depends on the atmospheric environment. Deforestation drives a shift toward more widespread, shallower clouds during the daytime, with amplified effects in dry inland areas compared with moist coastal regions. Aerosols only weakly modulate the cloud fraction response, but offset the cloud top height response to deforestation, suggesting the influence of aerosol indirect effects. We conclude that the local signature of forest loss is not uniform, and regional differences in climatology must be considered when assessing deforestation impacts on clouds and the climate system.

Plain Language Summary Humans are driving widespread deforestation in the tropics. Changes to the land surface following forest loss are generally known to affect the atmosphere, but it is hard to tell how deforestation will impact clouds in a given area. Here, we focus on Southeast Asia, a region of the world facing dramatic large-scale deforestation. We use two decades of satellite data to estimate how the loss of tropical forests impacts cloud properties. On average, we find that deforestation leads to more widespread and shallower clouds. We then look further into how this cloud response to deforestation depends on other environmental factors like moisture and aerosols. This gives us a better idea of which regions are most sensitive to changes in forest cover. Overall, our results show there is an observable cloud response to deforestation, but this response may be stronger in some regions than in others depending on underlying moisture and aerosol conditions. As forest loss continues in Southeast Asia and across the world, it is important to further study these region-dependent interactions between the atmosphere and the land surface so we can better understand the impacts of human-driven deforestation on weather and climate.

Key Points:

- Deforestation in Southeast Asia drives a robust shift toward more widespread and shallower clouds on an annual timescale
- This effect has been debated in modeling studies, but we demonstrate this observationally using two decades of satellite data
- Some regions are especially vulnerable to deforestation-driven changes in clouds, depending on atmospheric moisture and aerosol loading

Supporting Information:

Supporting Information may be found in the online version of this article.

Correspondence to:

G. R. Leung,
gabrielle.leung@colostate.edu

Citation:

Leung, G. R., Grant, L. D., & van den Heever, S. C. (2024). Deforestation-driven increases in shallow clouds are greatest in drier, low-aerosol regions of Southeast Asia. *Geophysical Research Letters*, *51*, e2023GL107678. https://doi.org/10.1029/2023GL107678

Received 4 DEC 2023
Accepted 14 APR 2024

Author Contributions:

Conceptualization: Gabrielle R. Leung, Susan C. van den Heever
Data curation: Gabrielle R. Leung
Formal analysis: Gabrielle R. Leung, Leah D. Grant, Susan C. van den Heever
Funding acquisition: Gabrielle R. Leung, Leah D. Grant, Susan C. van den Heever
Methodology: Gabrielle R. Leung
Project administration: Gabrielle R. Leung
Resources: Susan C. van den Heever
Software: Gabrielle R. Leung
Supervision: Leah D. Grant, Susan C. van den Heever
Validation: Gabrielle R. Leung

1. Introduction

Tropical forests are a key ecosystem component through their roles in carbon storage, the water cycle, and biodiversity (Gibson et al., 2011). However, these forests are at increasing risk of clearing or fragmentation across the globe due to anthropogenic activity (Kim et al., 2015; Song et al., 2018). Among the frontiers of tropical deforestation, Southeast Asia has had the most spatially pervasive and highest proportional rate of deforestation in recent years (Turubanova et al., 2018). Widespread logging and palm oil plantations in the region drove 16% forest cover loss between 2000 and 2020 (calculated as the percent difference in total forest cover fraction between the 2 years, Figure 1), despite increased government regulation of forest clearing (Margono et al., 2014).

Apart from the many damaging ecosystem and societal effects caused by deforestation, forest loss alters the biogeophysical properties of the land surface (Gentine et al., 2019). These land surface perturbations can propagate via surface fluxes to the atmosphere on local, regional, and even global scales (Gentine et al., 2019; Mahmood et al., 2014). Extensive prior studies show that deforestation leads to increases in near-surface temperatures by reducing evapotranspiration, increasing albedo, and reducing surface roughness (Crompton et al., 2021; Davin & de Noblet-Ducoudré, 2010). The impact of land surface changes on near-surface temperatures can be a similar magnitude to changes in global CO_2 concentrations in regions where land-atmosphere coupling is particularly strong, like in the tropics (Avila et al., 2012; Pitman et al., 2012). Land surface changes also impact the hydrological cycle—evaluating the local impacts of forest loss on clouds and precipitation is therefore crucial for managing water availability, especially given that almost half the global population lives in the tropics (Kummu & Varis, 2011). Furthermore, tropical clouds drive large-scale circulations and

Visualization: Gabrielle R. Leung
Writing – original draft: Gabrielle R. Leung
Writing – review & editing: Gabrielle R. Leung, Leah D. Grant, Susan C. van den Heever

impact global weather through teleconnections with other regions, which means changes in local convection due to deforestation in regions like Southeast Asia can have global consequences for weather and climate (Riehl & Malkus, 1958; Schneck & Mosbrugger, 2011; van der Molen et al., 2006).

Although the impact of deforestation on atmospheric temperature is broadly agreed upon, there remains uncertainty around the net impact of deforestation on convective clouds and precipitation (F. Chen & Avissar, 1994; Laguë et al., 2021). Many fine-scale processes driving land surface-convection feedbacks are not yet well-understood nor explicitly represented in climate models (Spracklen et al., 2018). As a result, the magnitude and even sign of reported deforestation impacts on clouds varies across model types and regions (Lawrence & Vandecar, 2015; Takahashi et al., 2017). In Southeast Asia, contrasting modeling studies have shown that deforestation leads to less clouds due to local drying (Tölle et al., 2017) or that deforestation leads to more clouds due to strengthened moisture transport (C.-C. Chen et al., 2019). Observational evidence of these land surface-convection feedbacks has been difficult to obtain due to relative sparsity of data (Lawrence & Vandecar, 2015) and difficulties in attributing measured impacts to land cover changes specifically. For example, rain gauge networks over parts of Southeast Asia have observed decreases in precipitation since the 1950's (Kanae et al., 2001), but there is debate about whether these changes are driven by deforestation or by other large-scale impacts on the regional climate (Tokinaga et al., 2012).

More recently, large satellite data sets have been used to estimate the cloud response to global forest losses (Duveiller et al., 2021; Teuling et al., 2017; Xu et al., 2022). For example, Xu et al. (2022) found a net increase in regional cloudiness over Southeast Asia associated with forest loss. However, in both these satellite-based studies and global modeling studies (Davin & de Noblet-Ducoudré, 2010; Findell & Eltahir, 2003; Winckler et al., 2017), the cloud response to deforestation varies seasonally and regionally. The exchanges of energy, moisture, and momentum that drive land-atmosphere interactions can be modulated by environmental properties (e.g., moisture availability, wind regimes) (Findell & Eltahir, 2003). The presence of aerosol particles absorbing and/or scattering radiation also alters the amount of radiation reaching the surface, and thus the partitioning of the surface energy budget (Jiang & Feingold, 2006; Leung & van den Heever, 2023). This can either dampen or strengthen cloud responses to surface perturbations depending on the aerosol loading (Grant & van den Heever, 2014; Park & van den Heever, 2022). In addition, aerosol particles can also interact with cloud microphysics, leading to synergistic or competing impacts in cloud properties relative to surface perturbations alone (Tao et al., 2012). The uncertainty surrounding the impact of deforestation on clouds is thus compounded by region-to-region variability in thermodynamic and aerosol environments.

In this paper, we use observations to demonstrate the impacts of long-term deforestation on cloud properties over Southeast Asia, and for the first time, examine the variability of these impacts as a function of environmental factors. This provides insight into which regions are at highest risk of deforestation-induced changes in convective clouds. As forest loss continues to accelerate in Southeast Asia and tropical forests around the globe, understanding the subsequent changes to clouds is essential to a fuller assessment of how future deforestation may impact humans and the broader earth system.

2. Data and Methods

We take forest cover observations from the Landsat-derived Global Forest Cover (GFC) data set (Hansen et al., 2013), which provides annual estimates of forest loss ($\Delta x \sim 30$ m). We utilize measurements of cloud fraction, cloud top height ($\Delta x \sim 1$ km), precipitable water (PWAT) vapor ($\Delta x \sim 1$ km), and aerosol optical depth (AOD, $\Delta x \sim 3$ km) from the Moderate Resolution Imaging Spectroradiometer (MODIS) (Platnick et al., 2017). MODIS observations are from the Terra and Aqua satellites with overpass times of ~10:30 a.m./p.m. and ~1:30 a.m./p.m., respectively, though PWAT and AOD are only available during daytime overpasses. To facilitate comparisons between the GFC and MODIS data sets, we resample and reproject the GFC data onto the same grid and resolution as the MODIS data and take annual averages of MODIS data to be at the same temporal resolution as the GFC data.

Changes in the cloud field from 1 year to another are driven by deforestation or by other sources of interannual variability (e.g., changes in the El Niño Southern Oscillation phase). Our approach leverages the large number of sample points using the "difference-in-differences" method (Crompton et al., 2021) to separate potential drivers of the observed cloud response. For each deforestation event, we take the change in cloud property between the year before and after the forest loss occurred. We compare the temporal change in cloud properties over deforested regions to the temporal change over a control intact forest group, which is near enough to experience

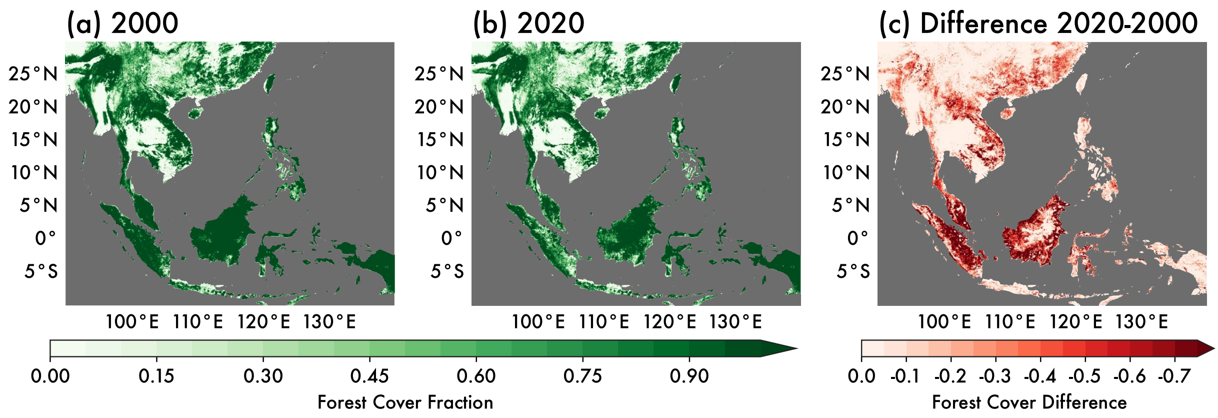

Figure 1. The fraction of forest cover in Southeast Asia in (a) 2000 and (b) 2020. (c) The difference in forest cover fraction (i.e., forest loss) between 2000 and 2020. Forest cover data are taken from the Global Forest Cover data set, as described in Section 2.

the same interannual variability but far enough away so as not to experience any direct impacts from the surface deforestation-induced perturbation (Figure S1 in Supporting Information S1). The difference between the response in deforested and control regions (represented by ε) can thus be interpreted as the response attributable to the forest loss alone. We then bootstrap an estimate of the mean ε over all sample points, aligning the response in time relative to the year in which the forest loss took place (Figures S2 and S3 in Supporting Information S1). The same response ε can be calculated for subsamples of the full population (Figures S3b and S3c in Supporting Information S1), which we group based on quartiles of environmental parameters, namely PWAT and AOD. Additional details can be found in Supporting Information S1.

Cloud response metrics are calculated at an annual timescale, given that forest cover is only available annually. Though this does not allow us to detect deforestation impacts on clouds at finer temporal scales (e.g., seasonal patterns), it does capture the integrated annual impact, which is most relevant to the radiative budget and the overall impact of deforestation on the climate system. We calculate the cloud response separately for each of the four overpass times to provide a picture of the diurnal variability in cloud responses to deforestation.

3. Results

3.1. Estimated Cloud Response to Deforestation

During the daytime (10:30 a.m. and 1:30 p.m.), increasing forest loss leads to an increase in the annual cloud fraction and a decrease in the mean cloud top height (Figure 2). In regions facing total forest loss, the annual mean

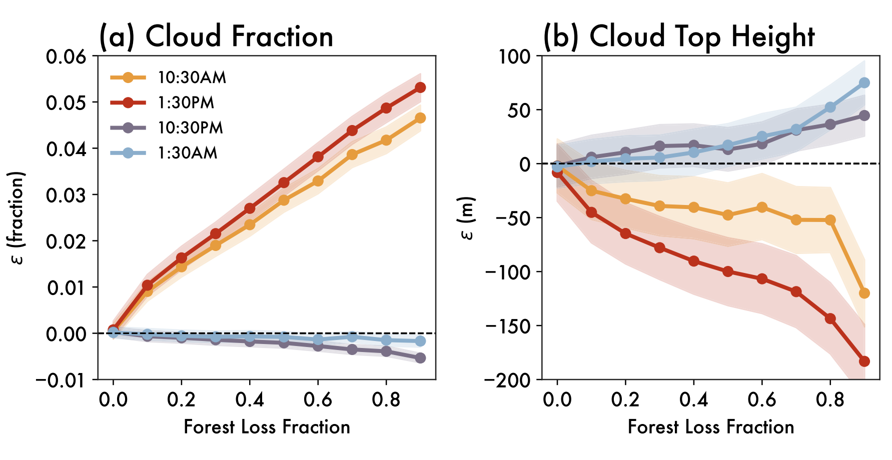

Figure 2. Estimated cloud response (ε) to mean forest loss for the annual mean (a) cloud fraction and (b) cloud top height (m). Different colored lines indicate different overpass times. Solid lines indicate the bootstrapped mean ($n = 1{,}000$), and shaded areas span the 25th to 75th percent confidence interval.

afternoon cloud fraction in the year following the deforestation event increases by up to 5% while the annual mean afternoon cloud top height is 200 m lower. Taken together, these changes indicate that the removal of forest cover leads to a local increase in coverage of shallow clouds. These results are generally consistent with findings from recent global satellite-based estimates of cloud responses to deforestation (Duveiller et al., 2021; Xu et al., 2022).

The magnitude of the cloud response to deforestation is largest during the afternoon (1:30 p.m.) and close to negligible at nighttime (10:30 p.m. and 1:30 a.m.) (Figure 2). This diurnal variation supports the hypothesis that changes in the cloud field following deforestation are driven by differential solar heating between forested and deforested regions. In the afternoon, the cloud response is largest, since surface heating has had sufficient time to drive strong mesoscale circulations and moisture transport. At night, the circulations and associated moisture transport into the deforested region is shut down and local moisture sources are no longer sufficient to support additional cloud development.

The daytime shift to more widespread shallow clouds following deforestation provides observational evidence for previously hypothesized mechanisms involving differential heating-driven mesoscale circulations and increased moisture transport (C.-C. Chen et al., 2019). Following a conversion from forest to bare soil, the reduction in soil moisture and evapotranspiration drives local drying (Werth & Avissar, 2005), which tends to hamper cloud formation. Deforestation may also lead to a reduction in biogenic volatile organic compound emissions, thereby reducing a potential source of cloud condensation nuclei (Duveiller et al., 2021). However, the anomalous local heating due to a combination of albedo, roughness, and moisture effects (Crompton et al., 2021) can induce mesoscale circulations that provide additional lift and transport moisture into the deforested area (Durieux et al., 2003; Wang et al., 2009). If the additional moisture source is sufficient, the combination of increased sensible heat fluxes due to a warmer surface and additional moisture due to mesoscale transport can support increased cloud formation. This has been demonstrated using models and observations for more well-studied regions like the Amazon (Khanna et al., 2017; Wang et al., 2009), but it has still been recently debated (C.-C. Chen et al., 2019; Lee & Lo, 2021) whether the same applies for Southeast Asia where land covers a much smaller fraction of the surface. This work provides observational evidence that deforestation in Southeast Asia causes more widespread and shallower clouds through effects on mesoscale circulations. Our findings support the more general hypothesis that tropical deforestation leads to increases in shallow clouds (Duveiller et al., 2021), at least for areas where there is an adequate moisture source nearby. Further work is still needed to explore the generality of this result for other tropical forests such as the inland Congo where moisture may be less readily available.

3.2. Modulation by Precipitable Water

To better understand the variability in cloud responses to deforestation, we segment the regional mean response (Figure 2) into environmental regimes (detailed in Supporting Information S1). Figure 3 explores deforestation-induced changes to cloud properties as modulated by PWAT vapor, the integrated amount of water vapor in the atmospheric column. Areas within the lowest PWAT quartile (∼48 mm) are generally inland or blocked by terrain, while regions in the highest PWAT quartile (∼57 mm) are typically coastal (Figures S4a and S4c in Supporting Information S1). It should be noted that the low and high PWAT divisions used here are relative terms, since even areas of Southeast Asia with lower PWAT are still in the humid tropics and have more moisture than arid continental areas.

We find the overall sign of cloud responses to deforestation do not depend on PWAT. That is, across all PWAT quartiles, regions with more forest loss tend to have higher cloud fractions and lower cloud top heights, and this effect is strongest in the afternoon. However, we do find that PWAT modulates the *magnitude* of the cloud response: the response to deforestation is stronger in dry regions than in moist regions or in Southeast Asia overall. Deforestation in drier inland Southeast Asia is thus expected to perturb cloudiness more than it would in the moist coastal areas.

The net deforestation impact on convection depends on a combination of local changes to moisture availability and mesoscale changes in lifting and moisture transport (Mahmood et al., 2014). We can assess the relative importance of these two processes based on the modulation of deforestation impacts by PWAT. The land surface in dry regions heats up faster than in moist regions, since less energy is needed to evaporate liquid water and drive latent heat fluxes. This leads to stronger thermal contrasts between forested and deforested regions, and thus stronger mesoscale circulations and increased mesoscale moisture transport. Although the deforested area sees a decrease in moisture available from local evapotranspiration, this is apparently outweighed by increased moisture

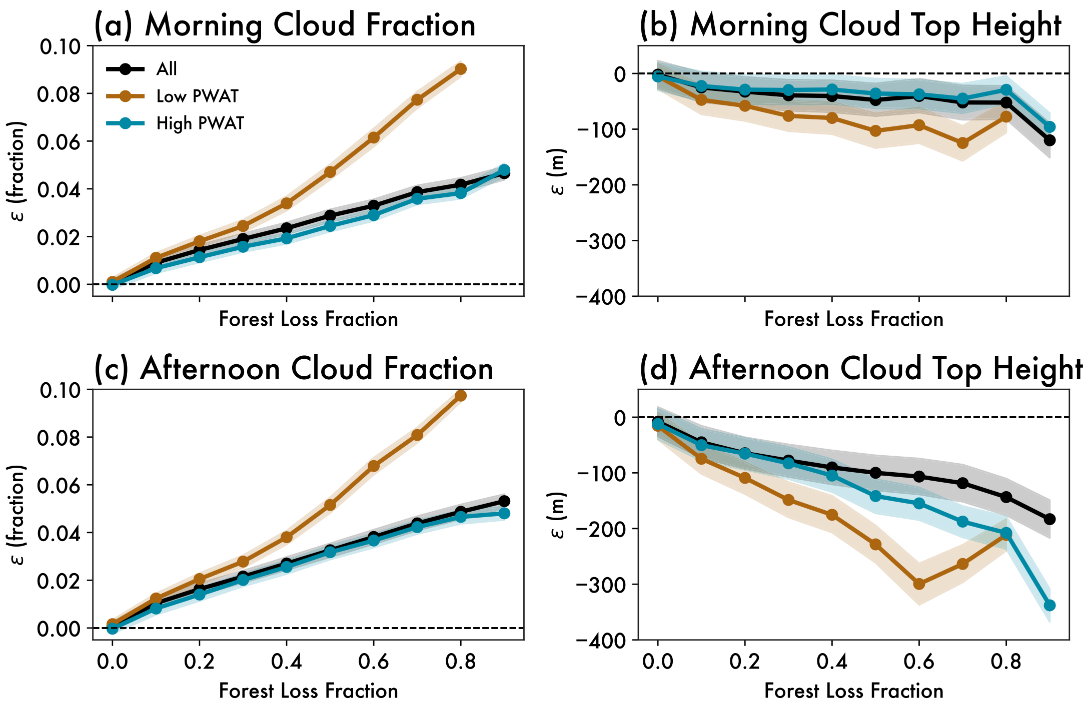

Figure 3. Dry regions experience enhanced deforestation impacts on cloud fraction and cloud top height. Data are segmented according to precipitable water quartile. (a, b) Show the Terra daytime overpasses (10:30 a.m.), and (c, d) show the Aqua daytime overpasses (1:30 p.m.). Lines and shading as in Figure 2.

from mesoscale transport. Because we see the cloud response to forest loss is strongest in low PWAT areas, our findings support that mesoscale transport is the dominant process by which deforestation impacts convection in Southeast Asia.

3.3. Modulation by Aerosol Optical Depth

In addition to the role of moisture in deforestation-cloud impacts, we examine the modulating role of aerosol loading. Figure 4 shows the cloud response to deforestation according to AOD, the integrated amount of light extinction by aerosol particles in the atmospheric column, which here serves as a satellite-observable proxy for aerosol loading. We focus here on AOD only, though we note that other factors more difficult to quantify from satellite data, such as aerosol type and spatial distribution, may also play a role. Areas in the low aerosol category have AODs below ∼0.2, while those in the high aerosol category have AODs above ∼0.4 (Figures S4b and S4d in Supporting Information S1). A higher AOD would result in less solar radiation reaching the surface, thus reducing the importance of surface perturbations on the overall circulation (Park & van den Heever, 2022).

Unlike with PWAT, we find the response of cloud *fraction* to deforestation is not strongly modulated by AOD. In both the morning and afternoon, low and high AOD categories are not statistically distinguishable from each other or the mean trend. This suggests that—for the range of AODs observed here—we do not expect a significant difference in deforestation impacts on cloud fraction between pristine and polluted environments.

On the other hand, AOD does modulate the sign and magnitude of the cloud top *height* response to forest loss, albeit to a lesser degree than PWAT (Figure 3). In the regional mean, annual cloud top height decreases with increasing forest loss, indicating a shift to shallower clouds. We find this is still true for the low AOD category. However, negligible or even positive increases in cloud top height are evident when AOD is high. Aerosol loading could therefore offset or mask the impacts of deforestation on cloud top heights. This modulation is consistent with past work showing that the presence of more numerous aerosol particles shifts the shallow cloud distribution toward higher cloud top heights (Leung et al., 2023; Spill et al., 2019; van den Heever et al., 2011). Though changes to cloud microphysics are difficult to ascertain from satellite measurements of AOD alone, these trends suggest that aerosol loading is an important modulator for deforestation-convection interactions.

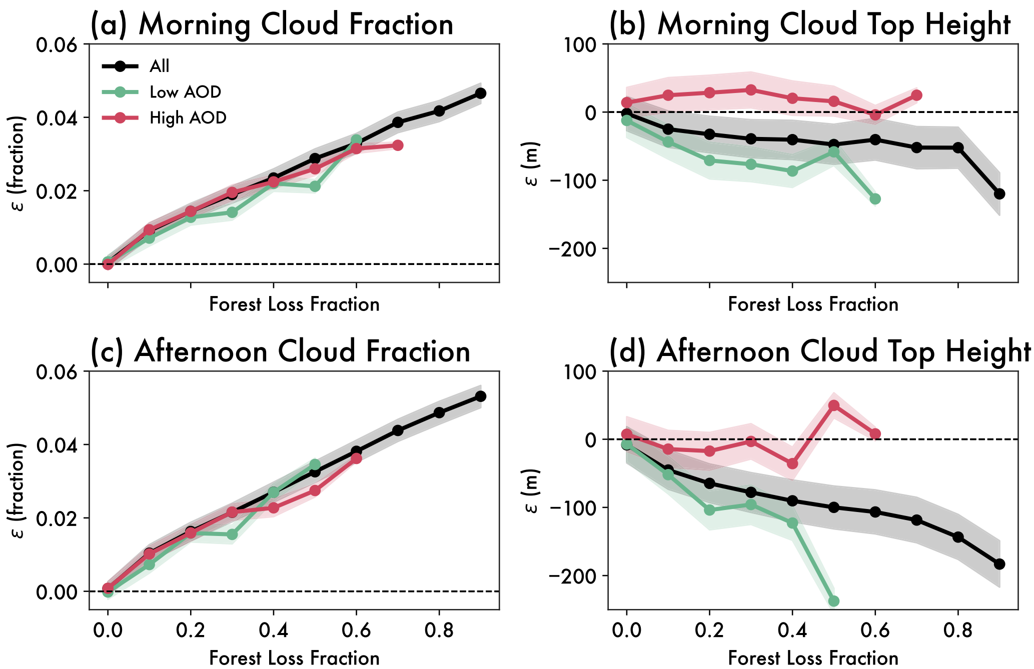

Figure 4. High aerosol loadings dampen deforestation impacts on cloud top height, but do not modulate deforestation-induced changes in cloud fraction. As in Figure 3, but segmented by aerosol optical depth quartile. Lines and shading as in Figure 2.

4. Conclusions

In conclusion, these results demonstrate there is a robust and detectable cloud response to deforestation in Southeast Asia on annual timescales and provides the first observational evidence that the magnitude of cloud responses depends on background atmospheric conditions. Mesoscale circulations between forested and deforested areas are likely the dominant mechanism for providing lift and transporting moisture, particularly in Southeast Asia where deforested areas are in close proximity to the ocean (Figures 5a and 5b). This study resolves past debates arising from regional modeling studies regarding whether cloudiness increases or decreases following deforestation. The increases in low cloud cover demonstrated here, to first order, exert a net cooling effect on the planet (L'Ecuyer et al., 2019). Through their influence on the radiative budget and the water cycle, these perturbations to tropical clouds can drive downstream climatic and societal impacts.

Moreover, we show for the first time that the magnitude of the observed cloud response to deforestation is strongly modulated by environmental factors like moisture and aerosol loading. Dry regions experience a stronger cloud response than moist regions (Figure 5c). Meanwhile, high aerosol loadings may mask the impact of deforestation on cloud top heights via offsetting impacts from the land surface changes and aerosol indirect effects (Figure 5d).

Future work should explore the sensitivity of the cloud response to deforestation to other environmental parameters that vary spatially, such as prevailing wind, atmospheric stability, differences in aerosol composition and vertical distribution, and soil type. Non-linear interactions between multiple parameters (e.g., simultaneously high PWAT and AOD) may further modulate the cloud response to deforestation. The current data set is insufficiently large to explore such multivariate relationships (Figure S3d in Supporting Information S1), though we recommend future work investigate such interactions once more data are available. Though this paper examined the cloud response to deforestation on annual timescales, once forest cover data are available at finer temporal resolutions, we also recommend that future analysis focus on understanding the seasonal variability of these impacts. We are currently exploring these complex land-atmosphere interactions using high-resolution numerical simulations, which also better allow for more certainty in the causal mechanism linking land cover changes and cloud responses.

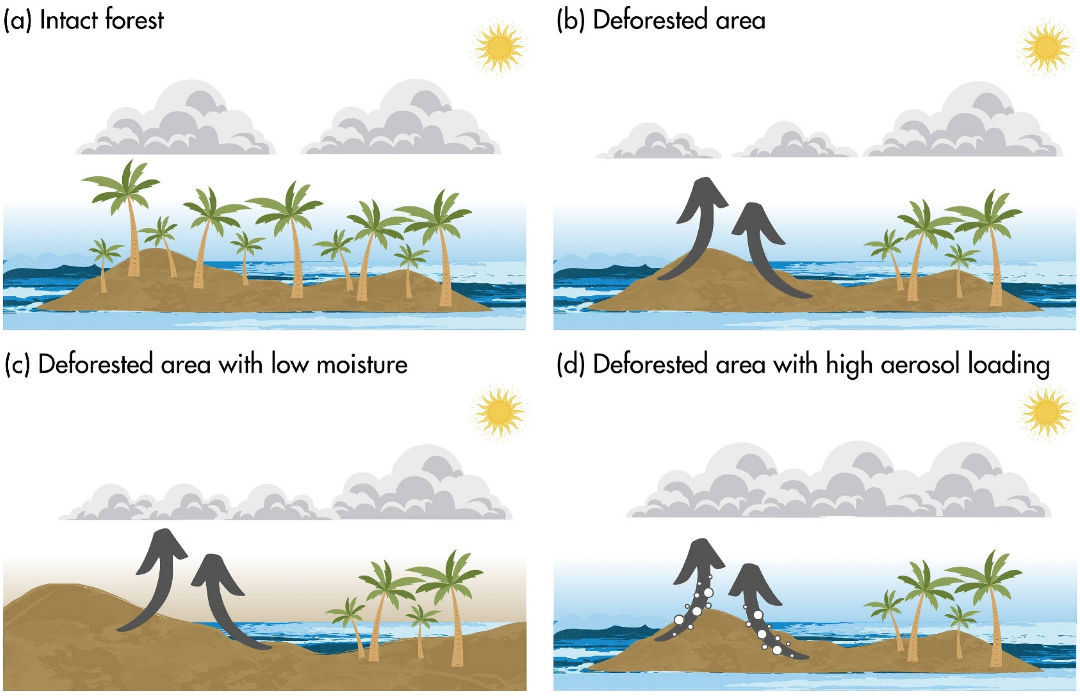

Figure 5. Schematic summarizing the impacts of deforestation on cloud properties in Southeast Asia, and modulation by moisture and aerosols. (a) Clouds forming over intact forest during daytime. (b) When an area is deforested, mesoscale circulations form (gray arrows) supporting shallow cloud development (more widespread coverage, but shallower on average in deforested areas compared to forested ones) by transporting moisture from nearby sources, such as oceans. (c) In an inland region with low atmospheric moisture locally available (represented by brown background gradient) but still in proximity to larger moisture sources such as the ocean, the impact of deforestation on clouds is magnified (even more widespread coverage and shallower clouds compared to panel (b)). (d) In a region with high aerosol loadings (white circles), the impact of deforestation on cloud fraction is the same (same coverage as panel (b)), but impacts on cloud top height are dampened (cloud top heights are similar between forested and deforested areas).

The results we describe here emphasize that the local signature of forest loss is not uniform, and that some areas are particularly susceptible to deforestation-driven changes in clouds due to climatological factors. Though often overlooked, taking variability in cloud responses to deforestation into account is essential for accurately assessing the impacts of deforestation on weather, hydrology, and future climates, especially as the rate of forest loss continues to accelerate in Southeast Asia and in tropical forests around the world.

Data Availability Statement

The UMD Global Forest Cover data are available at https://storage.googleapis.com/earthenginepartners-hansen/GFC-2022-v1.10/download.html. The MODIS cloud property data are available at Platnick et al. (2015b) (Aqua) and Platnick et al. (2015a) (Terra). The MODIS PWAT data are available at Borbas et al. (2017b) (Aqua) and Borbas et al. (2017a) (Terra). The MODIS AOD data are available at Levy and Hsu (2015b) (Aqua) and Levy and Hsu (2015a) (Terra). The EC JRC Global Surface Water data are available at https://global-surface-water.appspot.com/download. Processed data files used to generate the figures in this manuscript are available at Leung et al. (2024a). Analysis and plotting code are available at Leung et al. (2024b).

Acknowledgments

The authors would like to acknowledge that this research was supported by NASA FINESST Grant 80NSSC22K1446, NASA CAMP^{2}Ex Grant 80NSSC18K0149, and NSF Grant AGS-2029611.

References

Avila, F. B., Pitman, A. J., Donat, M. G., Alexander, L. V., & Abramowitz, G. (2012). Climate model simulated changes in temperature extremes due to land cover change. *Journal of Geophysical Research*, *117*(D4), D04108. https://doi.org/10.1029/2011JD016382

Borbas, E., Menzel, P., & Gao, B. (2017a). MODIS atmosphere L2 water vapor product (05_L2) [Dataset]. *NASA MODIS Adaptive Processing System, Goddard Space Flight Center*. https://doi.org/10.5067/MODIS/MOD05_L2.061

Borbas, E., Menzel, P., & Gao, B. (2017b). MODIS atmosphere L2 water vapor product (05_L2) [Dataset]. *NASA MODIS Adaptive Processing System, Goddard Space Flight Center*. https://doi.org/10.5067/MODIS/MYD05_L2.061

Chen, C.-C., Lo, M.-H., Im, E.-S., Yu, J.-Y., Liang, Y.-C., Chen, W.-T., et al. (2019). Thermodynamic and dynamic responses to deforestation in the maritime continent: A modeling study. *Journal of Climate*, *32*(12), 3505–3527. https://doi.org/10.1175/JCLI-D-18-0310.1

Chen, F., & Avissar, R. (1994). Impact of land-surface moisture variability on local shallow convective cumulus and precipitation in large-scale models. *Journal of Applied Meteorology and Climatology*, *33*(12), 1382–1401. https://doi.org/10.1175/1520-0450(1994)033<1382:IOLSMV>2.0.CO;2

Crompton, O., Corrêa, D., Duncan, J., & Thompson, S. (2021). Deforestation-induced surface warming is influenced by the fragmentation and spatial extent of forest loss in Maritime Southeast Asia. *Environmental Research Letters*, *16*(11), 114018. https://doi.org/10.1088/1748-9326/ac2fdc

Davin, E. L., & de Noblet-Ducoudré, N. (2010). Climatic impact of global-scale deforestation: Radiative versus nonradiative processes. *Journal of Climate*, *23*(1), 97–112. https://doi.org/10.1175/2009JCLI3102.1

Durieux, L., Machado, L. A. T., & Laurent, H. (2003). The impact of deforestation on cloud cover over the Amazon arc of deforestation. *Remote Sensing of Environment*, *86*(1), 132–140. https://doi.org/10.1016/S0034-4257(03)00095-6

Duveiller, G., Filipponi, F., Ceglar, A., Bojanowski, J., Alkama, R., & Cescatti, A. (2021). Revealing the widespread potential of forests to increase low level cloud cover. *Nature Communications*, *12*(1), 4337. https://doi.org/10.1038/s41467-021-24551-5

Findell, K. L., & Eltahir, E. A. B. (2003). Atmospheric controls on soil moisture–boundary layer interactions. Part I: Framework development. *Journal of Hydrometeorology*, *4*(3), 552–569. https://doi.org/10.1175/1525-7541(2003)004<0552:ACOSML>2.0.CO;2

Gentine, P., Massmann, A., Lintner, B. R., Hamed Alemohammad, S., Fu, R., Green, J. K., et al. (2019). Land–atmosphere interactions in the tropics – A review. *Hydrology and Earth System Sciences*, *23*(10), 4171–4197. https://doi.org/10.5194/hess-23-4171-2019

Gibson, L., Lee, T. M., Koh, L. P., Brook, B. W., Gardner, T. A., Barlow, J., et al. (2011). Primary forests are irreplaceable for sustaining tropical biodiversity. *Nature*, *478*(7369), 378–381. https://doi.org/10.1038/nature10425

Grant, L. D., & van den Heever, S. C. (2014). Aerosol-cloud-land surface interactions within tropical sea breeze convection. *Journal of Geophysical Research: Atmospheres*, *119*(13), 8340–8361. https://doi.org/10.1002/2014JD021912

Hansen, M. C., Potapov, P. V., Moore, R., Hancher, M., Turubanova, S. A., Tyukavina, A., et al. (2013). High-resolution global maps of 21st-century forest cover change. *Science*, *342*(6160), 850–853. https://doi.org/10.1126/science.1244693

Jiang, H., & Feingold, G. (2006). Effect of aerosol on warm convective clouds: Aerosol-cloud-surface flux feedbacks in a new coupled large eddy model. *Journal of Geophysical Research*, *111*(D1), D01202. https://doi.org/10.1029/2005JD006138

Kanae, S., Oki, T., & Musiake, K. (2001). Impact of deforestation on regional precipitation over the Indochina Peninsula. *Journal of Hydrometeorology*, *2*(1), 51–70. https://doi.org/10.1175/1525-7541(2001)002<0051:IODORP>2.0.CO;2

Khanna, J., Medvigy, D., Fueglistaler, S., & Walko, R. (2017). Regional dry-season climate changes due to three decades of Amazonian deforestation. *Nature Climate Change*, *7*(3), 200–204. https://doi.org/10.1038/nclimate3226

Kim, D.-H., Sexton, J. O., & Townshend, J. R. (2015). Accelerated deforestation in the humid tropics from the 1990s to the 2000s. *Geophysical Research Letters*, *42*(9), 3495–3501. https://doi.org/10.1002/2014GL062777

Kummu, M., & Varis, O. (2011). The world by latitudes: A global analysis of human population, development level and environment across the north–south axis over the past half century. *Applied Geography*, *31*(2), 495–507. https://doi.org/10.1016/j.apgeog.2010.10.009

Laguë, M. M., Swann, A. L. S., & Boos, W. R. (2021). Radiative feedbacks on land surface change and associated tropical precipitation shifts. *Journal of Climate*, *34*(16), 6651–6672. https://doi.org/10.1175/JCLI-D-20-0883.1

Lawrence, D., & Vandecar, K. (2015). Effects of tropical deforestation on climate and agriculture. *Nature Climate Change*, *5*(1), 27–36. https://doi.org/10.1038/nclimate2430

L'Ecuyer, T. S., Hang, Y., Matus, A. V., & Wang, Z. (2019). Reassessing the effect of cloud type on Earth's energy balance in the age of active spaceborne observations. Part I: Top of atmosphere and surface. *Journal of Climate*, *32*(19), 6197–6217. https://doi.org/10.1175/JCLI-D-18-0753.1

Lee, T.-H., & Lo, M.-H. (2021). The role of El Niño in modulating the effects of deforestation in the Maritime Continent. *Environmental Research Letters*, *16*(5), 054056. https://doi.org/10.1088/1748-9326/abe88e

Leung, G. R., Grant, L. D., & van den Heever, S. C. (2024a). Data associated with "Deforestation-driven increases in shallow clouds are greatest in drier, low-aerosol regions in Southeast Asia" [Dataset]. *Zenodo*. https://doi.org/10.5281/zenodo.10810714

Leung, G. R., Grant, L. D., & van den Heever, S. C. (2024b). GRLEUNG/SATLCC: Code associated with "deforestation-driven increases in shallow clouds are greatest in drier, low-aerosol regions in Southeast Asia" (v2.0-grl) [Software]. *Zenodo*. https://doi.org/10.5281/zenodo.10810757

Leung, G. R., Saleeby, S. M., Sokolowsky, G. A., Freeman, S. W., & van den Heever, S. C. (2023). Aerosol–cloud impacts on aerosol detrainment and rainout in shallow maritime tropical clouds. *Atmospheric Chemistry and Physics*, *23*(9), 5263–5278. https://doi.org/10.5194/acp-23-5263-2023

Leung, G. R., & van den Heever, S. C. (2023). Aerosol breezes drive cloud and precipitation increases. *Nature Communications*, *14*(1), 2508. https://doi.org/10.1038/s41467-023-37722-3

Levy, R., & Hsu, C. (2015a). MODIS atmosphere L2 aerosol product (04_3K) [Dataset]. *NASA MODIS Adaptive Processing System, Goddard Space Flight Center*. https://doi.org/10.5067/MODIS/MOD04_3K.061

Levy, R., & Hsu, C. (2015b). MODIS atmosphere L2 aerosol product (04_3K) [Dataset]. *NASA MODIS Adaptive Processing System, Goddard Space Flight Center*. https://doi.org/10.5067/MODIS/MYD04_3K.061

Mahmood, R., Pielke, R. A., Sr., Hubbard, K. G., Niyogi, D., Dirmeyer, P. A., McAlpine, C., et al. (2014). Land cover changes and their biogeophysical effects on climate. *International Journal of Climatology*, *34*(4), 929–953. https://doi.org/10.1002/joc.3736

Margono, B. A., Potapov, P. V., Turubanova, S., Stolle, F., & Hansen, M. C. (2014). Primary forest cover loss in Indonesia over 2000–2012. *Nature Climate Change*, *4*(8), 730–735. https://doi.org/10.1038/nclimate2277

Park, J. M., & van den Heever, S. C. (2022). Weakening of tropical sea breeze convective systems through interactions of aerosol, radiation, and soil moisture. *Atmospheric Chemistry and Physics*, *22*(16), 10527–10549. https://doi.org/10.5194/acp-22-10527-2022

Pitman, A. J., de Noblet-Ducoudré, N., Avila, F. B., Alexander, L. V., Boisier, J.-P., Brovkin, V., et al. (2012). Effects of land cover change on temperature and rainfall extremes in multi-model ensemble simulations. *Earth System Dynamics*, *3*(2), 213–231. https://doi.org/10.5194/esd-3-213-2012

Platnick, S., Ackerman, S., King, M., Meyer, K., Menzel, W., Holz, R., et al. (2015a). MODIS atmosphere L2 cloud product (06_L2) [Dataset]. *NASA MODIS Adaptive Processing System, Goddard Space Flight Center*. https://doi.org/10.5067/MODIS/MOD06_L2.006

Platnick, S., Ackerman, S., King, M., Meyer, K., Menzel, W., Holz, R., et al. (2015b). MODIS atmosphere L2 cloud product (06_L2) [Dataset]. *NASA MODIS Adaptive Processing System, Goddard Space Flight Center*. https://doi.org/10.5067/MODIS/MYD06_L2.006

Platnick, S., Meyer, K. G., King, M. D., Wind, G., Amarasinghe, N., Marchant, B., et al. (2017). The MODIS cloud optical and microphysical products: Collection 6 updates and examples from Terra and Aqua. *IEEE Transactions on Geoscience and Remote Sensing*, *55*(1), 502–525. https://doi.org/10.1109/TGRS.2016.2610522

Riehl, H., & Malkus, J. S. (1958). On the heat balance in the equatorial trough zone. *Geophysica*, *6*(3–4), 503–558.

Schneck, R., & Mosbrugger, V. (2011). Simulated climate effects of Southeast Asian deforestation: Regional processes and teleconnection mechanisms. *Journal of Geophysical Research*, *116*(D11), D11116. https://doi.org/10.1029/2010JD015450

Song, X.-P., Hansen, M. C., Stehman, S. V., Potapov, P. V., Tyukavina, A., Vermote, E. F., & Townshend, J. R. (2018). Global land change from 1982 to 2016. *Nature*, *560*(7720), 639–643. https://doi.org/10.1038/s41586-018-0411-9

Spill, G., Stier, P., Field, P. R., & Dagan, G. (2019). Effects of aerosol in simulations of realistic shallow cumulus cloud fields in a large domain. *Atmospheric Chemistry and Physics*, *19*(21), 13507–13517. https://doi.org/10.5194/acp-19-13507-2019

Spracklen, D. V., Baker, J. C. A., Garcia-Carreras, L., & Marsham, J. H. (2018). The effects of tropical vegetation on rainfall. *Annual Review of Environment and Resources*, *43*(1), 193–218. https://doi.org/10.1146/annurev-environ-102017-030136

Takahashi, A., Kumagai, T., Kanamori, H., Fujinami, H., Hiyama, T., & Hara, M. (2017). Impact of tropical deforestation and forest degradation on precipitation over Borneo Island. *Journal of Hydrometeorology*, *18*(11), 2907–2922. https://doi.org/10.1175/JHM-D-17-0008.1

Tao, W.-K., Chen, J.-P., Li, Z., Wang, C., & Zhang, C. (2012). Impact of aerosols on convective clouds and precipitation. *Reviews of Geophysics*, *50*(2), RG2001. https://doi.org/10.1029/2011RG000369

Teuling, A. J., Taylor, C. M., Meirink, J. F., Melsen, L. A., Miralles, D. G., van Heerwaarden, C. C., et al. (2017). Observational evidence for cloud cover enhancement over western European forests. *Nature Communications*, *8*(1), 14065. https://doi.org/10.1038/ncomms14065

Tokinaga, H., Xie, S.-P., Timmermann, A., McGregor, S., Ogata, T., Kubota, H., & Okumura, Y. M. (2012). Regional patterns of tropical Indo-Pacific climate change: Evidence of the walker circulation weakening. *Journal of Climate*, *25*(5), 1689–1710. https://doi.org/10.1175/JCLI-D-11-00263.1

Tölle, M. H., Engler, S., & Panitz, H.-J. (2017). Impact of abrupt land cover changes by tropical deforestation on Southeast Asian climate and agriculture. *Journal of Climate*, *30*(7), 2587–2600. https://doi.org/10.1175/JCLI-D-16-0131.1

Turubanova, S., Potapov, P. V., Tyukavina, A., & Hansen, M. C. (2018). Ongoing primary forest loss in Brazil, Democratic Republic of the Congo, and Indonesia. *Environmental Research Letters*, *13*(7), 074028. https://doi.org/10.1088/1748-9326/aacd1c

van den Heever, S. C., Stephens, G. L., & Wood, N. B. (2011). Aerosol indirect effects on tropical convection characteristics under conditions of radiative–convective equilibrium. *Journal of the Atmospheric Sciences*, *68*(4), 699–718. https://doi.org/10.1175/2010JAS3603.1

van der Molen, M. K., Dolman, A., Waterloo, M., & Bruijnzeel, L. (2006). Climate is affected more by maritime than by continental land use change: A multiple scale analysis. *Global and Planetary Change*, *54*(1–2), 128–149. https://doi.org/10.1016/j.gloplacha.2006.05.005

Wang, J., Chagnon, F. J. F., Williams, E. R., Betts, A. K., Renno, N. O., Machado, L. A. T., et al. (2009). Impact of deforestation in the Amazon basin on cloud climatology. *Proceedings of the National Academy of Sciences of the United States of America*, *106*(10), 3670–3674. https://doi.org/10.1073/pnas.0810156106

Werth, D., & Avissar, R. (2005). The local and global effects of Southeast Asian deforestation. *Geophysical Research Letters*, *32*(20), L20702. https://doi.org/10.1029/2005GL022970

Winckler, J., Reick, C. H., & Pongratz, J. (2017). Robust identification of local biogeophysical effects of land-cover change in a global climate model. *Journal of Climate*, *30*(3), 1159–1176. https://doi.org/10.1175/JCLI-D-16-0067.1

Xu, R., Li, Y., Teuling, A. J., Zhao, L., Spracklen, D. V., Garcia-Carreras, L., et al. (2022). Contrasting impacts of forests on cloud cover based on satellite observations. *Nature Communications*, *13*(1), 670. https://doi.org/10.1038/s41467-022-28161-7

References From the Supporting Information

Frey, R. A., Ackerman, S. A., Liu, Y., Strabala, K. I., Zhang, H., Key, J. R., & Wang, X. (2008). Cloud detection with MODIS. Part I: Improvements in the MODIS cloud mask for collection 5. *Journal of Atmospheric and Oceanic Technology*, *25*(7), 1057–1072. https://doi.org/10.1175/2008JTECHA1052.1

Kaufman, Y. J., & Gao, B.-C. (1992). Remote sensing of water vapor in the near IR from EOS/MODIS. *IEEE Transactions on Geoscience and Remote Sensing*, *30*(5), 871–884. https://doi.org/10.1109/36.175321

Levy, R. C., Mattoo, S., Munchak, L. A., Remer, L. A., Sayer, A. M., Patadia, F., & Hsu, N. C. (2013). The Collection 6 MODIS aerosol products over land and ocean. *Atmospheric Measurement Techniques*, *6*(11), 2989–3034. https://doi.org/10.5194/amt-6-2989-2013

Pekel, J. F., Cottam, A., Gorelick, N., & Belward, A. S. (2016). High-resolution mapping of global surface water and its long-term changes. *Nature*, *540*(7633), 418–422. https://doi.org/10.1038/nature20584

Strabala, K. I. (2004). MODIS cloud mask user's guide. Retrieved from http://cimss.ssec.wisc.edu/modis1/pdf/CMUSERSGUIDE.PDF